ISSN 0036-0295, Russian Metallurgy (Metally), Vol. 2013, No. 9, pp. 706–711. © Pleiades Publishing, Ltd., 2013.
Original Russian Text © L.A. Maltseva, Yu.N. Loginov, T.V. Maltseva, V.A. Sharapova, 2013, published in Metally, 2013, No. 5, pp. 85–92.

Effect of the State of Stress on the Strain-Induced Martensite Formation in 03Kh14N11K5M2YuT Steel[1]

L. A. Maltseva*, Yu. N. Loginov, T. V. Maltseva, and V. A. Sharapova

Ural Federal University (UrFU), Yekaterinburg, Russia

**e-mail: mla44@mail.ru*

Received November 14, 2012

Abstract—The structural changes that occur in a metastable austenitic Fe–Cr–Ni–based steel during cold plastic deformation by drawing and tension are analyzed. A relation between the structure of the steel and its mechanical and magnetic properties is established. It is concluded that the stress state scheme considerably affects the rate of martensite formation.

DOI: 10.1134/S0036029513090097

INTRODUCTION

12Kh18N10T steel is used in industry for elastic elements and certain types of medical instrument. It has a number of disadvantages: reduced relaxation resistance and lack of ductility and workability, which leads to a large number of intermediate annealings in wire drawing (especially for thin wires).

A new corrosion-resistant austenitic steel (03Kh14N11K5M2YuT) was developed at the Department of Metallurgy in UrFU [1, 2]. The developed steel is practically carbon-free. The carbon content is no more than 0.02–0.03%. This provides high plasticity and manufacturability in the quenched state. As shown in [3, 4], the presence of metastable strain-induced austenite and the pronounced trip-effect in the steel make it possible to use severe plastic deformation during wire drawing and to form a nanocrystalline structure in the steel. As a result, the strength properties increase by 4–5 times. The investigated steel can retain a high ductility at the stages of pressure processing. This can significantly decrease the number of intermediate annealings during the production of thin wires and, thus, reduces the product costs even at such a high doping level.

To form high-level properties, the evolution of martensitic transformations during deformation should be controlled in order to optimize the steel structure. As was shown in [5–9], the level of accumulated strain affects the formation of strain-induced martensite, and the consideration of the stress state scheme is also important. American and French researchers from the Massachusetts Institute of Technology and Ecole Polytechnique [6] proposed to describe the kinetics of the austenite–martensite transformation using the Lode strain parameter, i.e., the stress triaxiality. At the same plastic strain, the martensite content in steel SS301LN is higher in the transition from a uniaxial compression scheme to uniaxial tension.

The authors of [6] present the results of [7] as a confirmation of these findings: South Korean researchers from the Institute of Machinery and Materials refer to the data showing a significant effect of the strain rate on the kinetics of martensitic transformation [8]. For example, the amount of the martensitic phase, which induced by a true strain of 0.4 with strain rate increasing from 0.00013 to 0.13 s^{-1}, decreases from 70 to 15%, i.e., more than 4 times. Accordingly, the strain rate acts as an abnormal softening factor: the strengthening curves of the material deformed at a high strain rate are below the curves of the material deformed at a lower strain rate.

Thus, changes in the scheme and parameters of the strain and stress state of the selected class of materials leads to a significant change in their properties.

The purpose of this study is to investigate the influence of the stress state in an Fe–Cr–Ni steel during tension and drawing on the intensity of strain-induced formation martensite.

EXPERIMENTAL

The study was carried out on steel 03Kh14N11K5M2YuT with the following chemical composition (wt %): ~0.02 C; 14.2 Cr; 11.4 Ni; 4.5 Co; 2.2 Mo; 0.83 Al; 0.4 Ti; total S, P, and Cu ≤0.035; and Fe for balance.

Preparation of Samples

Bars were forged and ground to a diameter of 14 mm after melting in induction furnaces and homogenizing annealing at 1160°C for 10 h. The initial workpiece was heat treated according to following

[1] The article was translated by the author.

regime: heating to 1000–1050°C and quenched in water to fix the soft state. Pickling was carried out in a solution of concentrated acid for 30 min. The samples were washed and dried to prepare the surface for coating. Preform was thinned by drawing to a diameter of 14 mm to obtain an intermediate size wire. Stainless steels have high adhesion to the drawing tool. Therefore, before drawing a lubricant layer was deposited by liming: a wire was repeatedly immersed in a solution of lime with intermediate drying and then subjected to final drying at room temperature.

Wire samples were drawn in a multiple universal UIM 10 testing machine with an attachment for fixing drawing dies and moving speed clamp of 20 mm/min. Samples were taken on the drawing test as wire pieces. The dies were made of VK6 hard alloy (tungsten carbide + 6% cobalt) and had a working cone angle of 6°, and sodium soap powder was used as a lubricant.

Microstructural Studies

They were carried out on an OLYMPUS JX-51 optical microscope at magnifications of 200 and 500-fold. Electron microscopy studies were performed on JEM-200CX and JSM-5610LV microscopes.

Mechanical Testing

Tensile specimens were tested on Instron 3382 testing machine to record stress–strain curves and at a clamp movement speed of 10 mm/min. Ultimate strength σ_u, yield strength $\sigma_{0.2}$, and elongation to failure δ were determined according to GOST 1497–84.

Measurements of the Magnetic Characteristics

The magnetic characteristics of the samples were measured during elastic–plastic deformation by tension on the installation included a computerized Remagraph C-500 hysteresisgraph and an upgraded UMM-5 testing machine and on a DRON-2 diffractometer using Co$K\alpha$ (or Cr$K\alpha$) radiation.[2] The contents of the bcc and fcc phases were determined using homologous pairs.

Texture Analysis[3]

The measurements were performed using inverse pole figures constructed with a diffractometer. X-ray diffraction spectra were recorded with an automated DRON 4 diffractometer using monochromatic Co$K\alpha$ radiation for quantitative phase analysis. Recording was performed in the angular range $2\theta = 10°–130°$ in increments of 0.1° and an exposure of 3–5 seconds at each point in the Bragg–Brentano geometry. For monochromatisation, a graphite monochromator was used. Processing of the spectra was carried out using the software package developed at the Department of Physical Material Science in MISiS [10]. The error in the determination of the lattice parameters was 0.003–0.004 Å. The relative error in the determination of the volume fractions was less than 5%.

RESULTS AND DISCUSSION

Initial State

The initial quenched state was studied by microstructural analysis. The microstructure of the investigated steel after quenching from 1000°C is conventional for austenitic steels: austenitic grains have a polyhedral shape with a size up to 30 microns and a large number of annealing twins (Figs. 1a, 1b). The microhardness of austenite was ~*HV* 190–200.

Mechanical Properties

The wire 4.0 mm in diameter fabricated by repeated drawing was subjected to softening heat treatment (quenching from 1000°C in water). After the tension of samples on the test machine, the following plasticity characteristics were obtained: the uniform elongation was 44%, the total elongation was 64%, the relative reduction of area was 83%, ultimate strength was $\sigma_u = 540$ MPa, and the yield strength was $\sigma_{0.2} = 245$ MPa.

To estimate the strain state of the wire, we used alternative approaches. In materials science, researchers use relative elongation $\varepsilon_l = 100(l_1 - l_0)/l_0$ or relative reduction of area $\varepsilon_F = 100(F_0 - F_1)/F_0$. Here, l_0, l_1, F_0, and F_1 are the length and the cross-sectional area of the base portion of the sample before and after deformation, respectively.

For low strains (5%), the differences between these quantities are negligible. However, the discrepancy is significant at higher strains. Therefore, the true strain (sometimes called logarithmic strain) is additionally applied,

$$\varepsilon = \ln(F_0/F_1). \quad (1)$$

The use of this parameter allowed us to summarize these quantities using multipass deformation schemes, which cannot be done using indices ε_l and ε_F.

The experimental results obtained with the help of mathematical processing were used to plot true stress σ versus relative reduction of area ε_F and (logarithmic) strain ε (Figs. 2a, 2b).

[2] We thank S.M. Zadvorkin, Institute of Mechanical Engineering, Ural Branch, Russian Academy of Sciences, for assistance.
[3] We are grateful to T.A. Sviridova, CCU National Research Technological University MISiS, for assistance in the measurement of texture in the investigated steels.

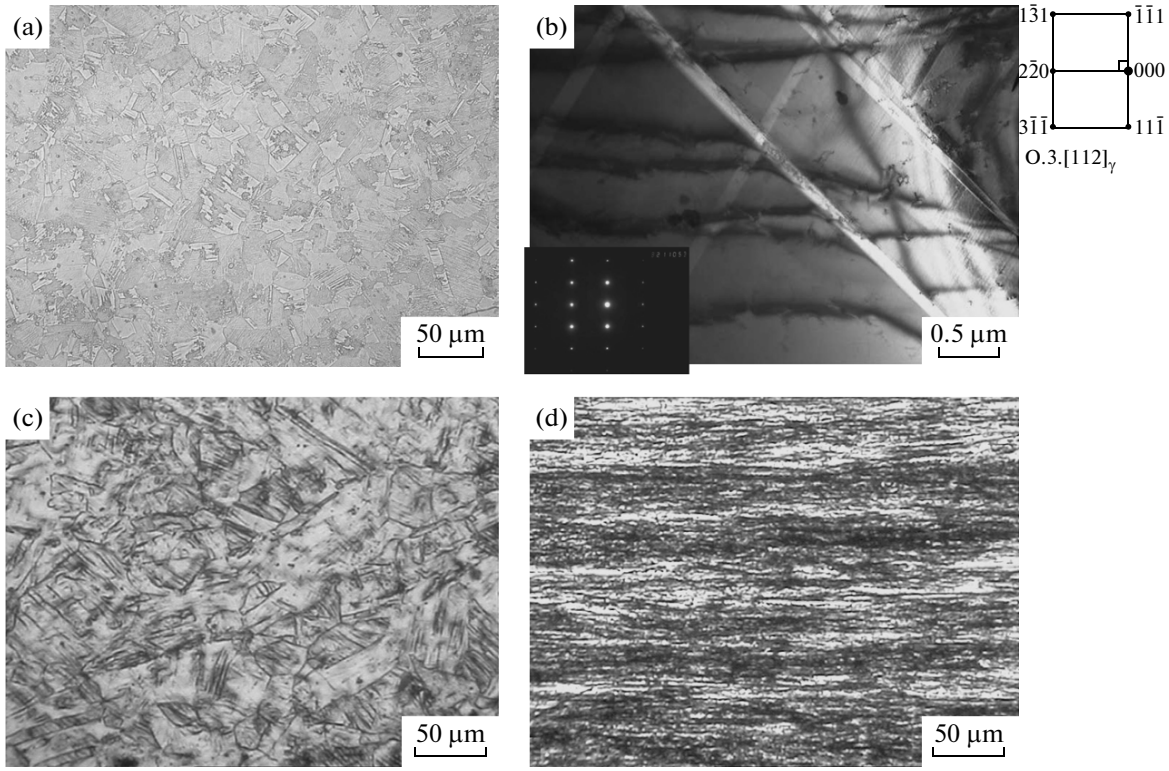

Fig. 1. Microstructure of (a, b) quenched and (c, d) deformed 03Kh14N11K5M2YuT steel at true strain (c) $\varepsilon = 0.52$ and (d) $\varepsilon = 2.32$.

Mathematical Processing of the Strain State Indices

The resulting loading diagram was approximated by the method of least squares and the regression equations (in MPa)

$$\sigma = 245 + 93.4\varepsilon_F^{0.538}, \quad (2)$$

$$\sigma = 245 + 986\varepsilon^{0.500}, \quad (3)$$

were derived.

The first term in these equations is the yield strength for the not cold-worked state of the metal, i.e., $\sigma_{0.2} = 245$ MPa.

The second stage of the study was repeated drawing of the wire as described above with sampling and determination of the standard characteristics, including the yield strength. The yield strength is interpreted as the stress corresponding to the start of plastic deformation of the metal.

In continuum mechanics, the yield strength is often compared to the concept of resistance to deformation, which allows one to obtain a relation between the flow stress and the strain, i.e., to trace how a metal is strengthened during deformation. Therefore, it is necessary to determine the characteristic of work hardening for drawing.

In the Russian technical literature, strain ε_0 is usually applied to assess the state of stress in drawing, which is typically associated with the reduction ratio,

$$\varepsilon_0 = \ln\lambda_i = 2\ln(d_{i-1}/d_i), \quad (4)$$

where d_{i-1} and d_i are the wire diameters before and after the drawing die in the current pass that is carried out with reduction ratio λ_i.

As can be seen from a comparison of Eqs. (1) and (4), indices ε and ε_0 are estimated according to the same formulas. However, this strain during drawing is only imparted by the axial area of the wire at radial coordinate $r = 0$, since it is deformed under uniaxial tension conditions due to a decrease in the diameter and the trajectory of its movement is a straight line. The strains in the peripheral part of the wire are higher due to the additional shears imparted by the metal because of a change in the trajectory of motion through the die. Therefore, $\varepsilon \neq \varepsilon_0$ in more accurate calculations.

The authors of [11] referred to [12] and proposed to estimate the additional shear strain during drawing using the formula for calculating the strain averaged over the cross section,

$$\varepsilon_{av} = \phi\varepsilon_0. \quad (5)$$

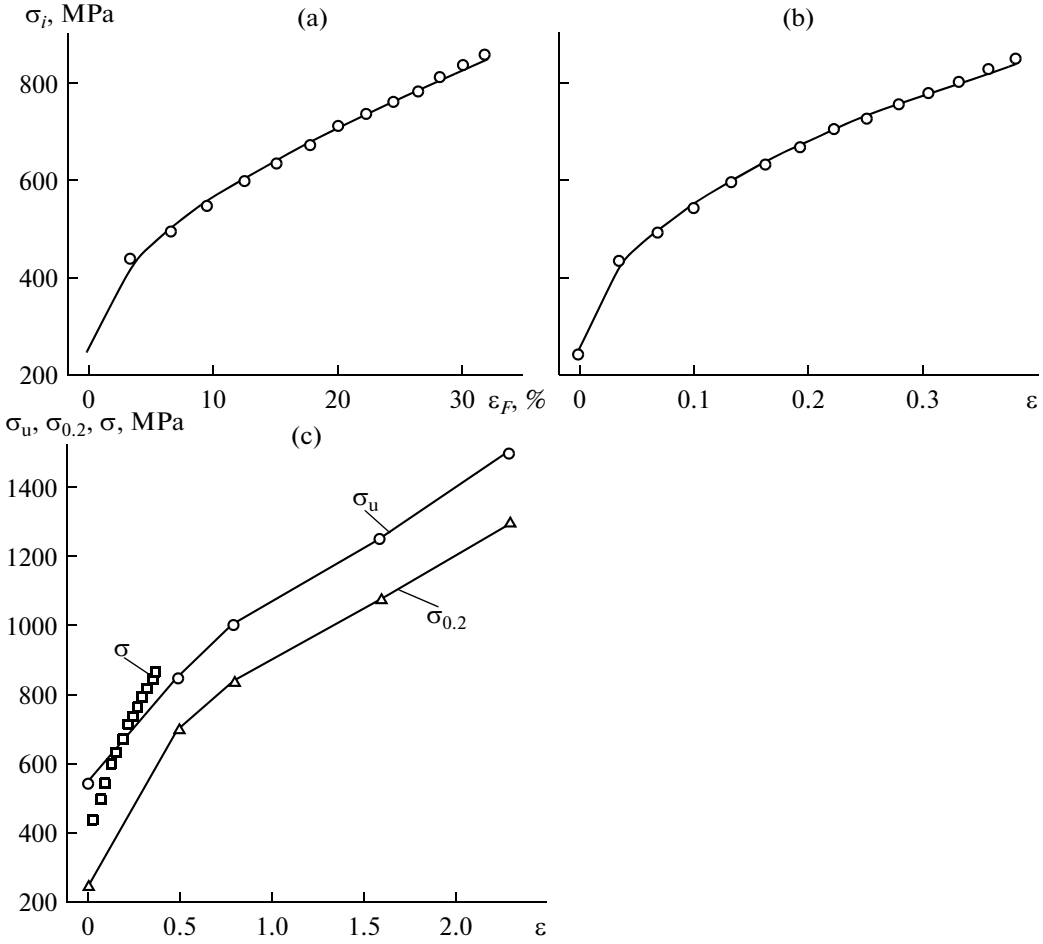

Fig. 2. True stress σ_i vs. (a) relative reduction of area ε_F and (b) strain ε (logarithmic strain). (c) Ultimate tensile strength σ_u, yield strength $\sigma_{0.2}$, and plastic flow stress σ vs. strain ε. (points) Experimental data for 03Kh14N11K5M2YuT steel and (lines) calculation by a regression equation

Here ϕ is the additional strain factor dependent on the type of material. In particular, the following formula is used for the class of stainless steels:

$$\phi = 0.87 + 0.15\Delta,$$

where Δ is the parameter interpreted as the ratio of the drawing die diameter to the length of the contact deformation zone surface,

$$\Delta = \frac{1 + \sqrt{1 - \varepsilon_0/100}}{1 - \sqrt{1 - \varepsilon_0/100}} \sin\alpha,$$

where α is the slope of the generatrix of the drawing die.

During repeated drawing, cumulative strain in the current pass is determined by the formula

$$\varepsilon_{\Sigma n_{av}} = \sum_{1}^{n} \varepsilon_{iav},$$

where ε_{iav} is the partial strain in the pass with allowance for additional shears. The resulting cumulative strain can be considered as a quantity independent of the load application scheme; i.e., we can assume $\varepsilon = \varepsilon_{\Sigma n_{av}}$ and, thus, are able to compare the deformation effect during both tension and drawing.

Such a comparison is shown in Fig. 2c. It can be seen that the metal is subjected to intense work hardening: when the strain is 2.3, the yield strength increases from 245 to 1300 MPa, i.e., by more than 5 times, and the ultimate strength increases from 540 to 1500 MPa, i.e., by about 3 times.

In particular, the difference in yield stress increases during tension and drawing. In linear tension, the stresses are higher than upon drawing; that is, the material exhibits higher strength properties.

This phenomenon can be explained by the fact that, in a linear state of stress, the martensitic transformation in the steel is more intense. Figure 3 schematically shows the nature of the state of stress in the metal during linear tension and drawing. In tension along the axis of the specimen, only stress σ_{zz} acts. In drawing, the following compressive stresses are added: radial σ_{rr}

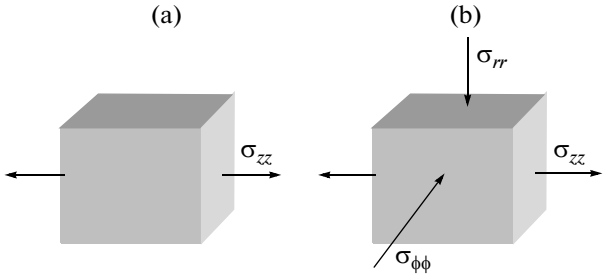

Fig. 3. Stresses for the linear state of stress during (a) tension and (b) drawing.

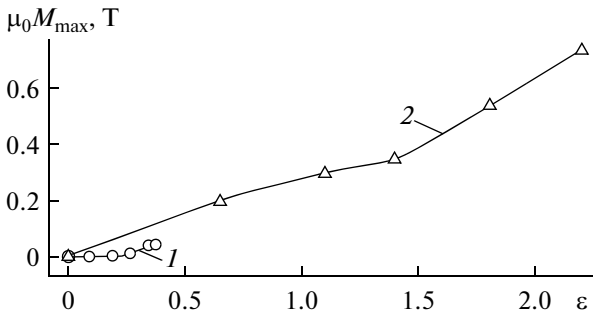

Fig. 4. Magnetization of 03Kh14N11K5M2YuT steel vs. the strain during (*1*) tension and (*2*) drawing.

and tangential $\sigma_{\phi\phi}$ from the die walls, which leads to a shift of the hydrostatic stress $\sigma = (\sigma_{zz} + \sigma_{rr} + \sigma_{\phi\phi})/3$ to the compressive state of stress.

Many researchers associate the martensitic transformation as a result of plastic deformation with the scheme of the stress state. For example, based on experimental results, the authors of [6] placed stress state schemes according to an increase in the rate of martensitic transformation in the following order: equiaxed compression, shear, uniaxial compression, and uniaxial tensile. One can see that the schemes are placed according to an increase in the tensile stress, which is consistent with our results.

Note that the single curve hypothesis accepted in the mechanics of deforming bodies does not hold true for steels with martensite induced by plastic deformation. According to this hypothesis, the shape of a plastic flow curve is independent of the stress state scheme. These and other experiments showed that the yield stress is shifted to higher values at a greater amount of martensite in steels with strain-induced martensite. The intensity of its formation depends on the stress state scheme.

Magnetic Tests

The strain state for magnetic tests, as in the previous case, was achieved in the following two ways: tension of wire samples and their drawing. The deformed state scheme is identical in these two methods: tensile strains occur in the direction of increasing length, and compression strains are produced in the transverse direction. In this case, the stress state is different: only tensile stresses act under tension, and compressive stresses in orthogonal directions are added to them during drawing.

Thus, in one case, the wire was tensioned in the initial state with continuous tracing of the magnetic characteristics in a Remagraph C-500 magnetic measuring complex. In the other case, samples were first deformed by drawing to a specific strain, and the magnetic properties were then measured on a DRON-2 X-ray diffractometer.

An increase in magnetization $\mu_0 M_{max}$ (where $\mu_0 = 4\pi \times 10^{-7}$ H is the magnetic constant) is observed in tension of the investigated steels in the Remagraph C-500 magnetic measuring complex. The increase in the magnetization indicates an increase in the content of the magnetic phase, i.e., strain-induced α martensite. Figure 4 shows the magnetization of steel 03Kh14N11K5M2YuT during uniaxial tension (short line *1* due to rupture of the sample) and drawing for the same indices of the deformed state. It is seen from these curves that a more intense increase of the magnetic properties is observed at high accumulated strains.

X-ray Diffraction Analysis

X-ray diffraction analysis of steel 03Kh14N11K5M2YuT samples showed that the content of the bcc phase (δ ferrite and α martensite) increased to 63% after rupture in a tensile test.

Phase and Texture Analyses

Microstructural studies of the deformed wire samples tensioned to a deformation $\varepsilon = 4.15$ were carried out to determine the effect of strain on the structure of the steel. Slip bands appear at moderate degrees of deformation in individual grains, and the grain shape changes at high degrees of deformation: equiaxed grains change into more fibrous, elongated along the deformation axis (Figs. 1c, 1d).

An axial texture forms in the process of cold drawing of the steel. Basic ⟨111⟩ orientation occurs in the austenitic matrix at moderate strains. The volume fraction of martensite in the structure becomes noticeable at strains higher than $\varepsilon = 1.15$, and the preferential orientation of α-solid solution crystals occurs in the ⟨100⟩ direction. Densities are specified for the orientation poles of the steel after cold plastic deformation with different degrees of drawing for texture acuteness evaluation (table). The pole densities indicate a significant increase in the acuteness texture at increasing deformation as compared to the sample

Quantitative analysis and texture of 03Kh14N11K5M2YuT steel after cold plastic deformation by drawing at various reductions ε

ε	Phase	ω_V	ω_m	a, nm	Basic orientation/Pole density
		%			
1.15	α	25.8 ± 0.3	25.4 ± 0.3	0.2874	$\langle 110\rangle/P_{110} = 1.8$
	γ	74.2 ± 0.3	74.6 ± 0.3	0.3592	$\langle 100\rangle$ and $\langle 111\rangle/P_{100} = 1.8$, $P_{111} = 1.5$
2.99	α	84.3 ± 0.3	84.0 ± 0.3	0.2878	$\langle 110\rangle/P_{110} = 2.2$
	γ	15.7 ± 0.3	16.0 ± 0.3	0.3598	–
4.15	α	92.9 ± 0.2	92.7 ± 0.2	0.2878	$\langle 110\rangle/P_{110} = 2.9$
	γ	7.1 ± 0.2	7.3 ± 0.2	0.3602	–

ω_V and ω_m are the volume and mass fractions of the phases, respectively, and a is the lattice parameter.

without texture; i.e., the larger the deviation of the pole density from unity, the sharper the texture.

Analysis of the pole density and the volume fraction of martensite shows that the amount of strain-induced martensite and the pole density of α martensite increases continuously with the degree of deformation by drawing.

The study of the evolution of structure in steel during deformation [4] showed that the scheme of martensitic transformation in drawing is $\gamma \rightarrow \varepsilon \rightarrow \alpha$. Microtwinning and ε-martensite areas are retained until $\varepsilon = 0.5$. Active formation of α martensite is observed in the investigated steel at strain more than $\varepsilon = 0.9$. The intensity of the martensite formation increases with the strain. The amount of martensite upon deformation at $\varepsilon \approx 4.15$ exceeds 90%. It is known that martensitic transformation facilitates plastic deformation due to the elimination of local peak stresses. This leads to high ductility and workability, at such high degrees of compression.

The practical value of the work is to establish a relation between the state of stress and the intensity of deformation-induced martensite formation in 03Kh14N11K5M2YuT steel. That allows one to create industrial metal processing schemes with more intense strain hardening of a material.

CONCLUSIONS

(1) The intensity of strain-induced martensite formation depends on the stress state scheme in the process of deformation processing of 03Kh14N11K5M2YuT steel.

(2) Is revealed that the rate of martensite formation under uniaxial tensile stress state is higher than for the bulk stress state drawing scheme at equal levels of strains.

(3) At a true strain of 2.3, the yield strength of the steel can increase more than fivefold and the ultimate strength increases about threefold.

(4) At $\varepsilon \approx 4.15$, the amount of strain-induced martensite exceeds 90%, and the preferred orientation of α-solid solution crystals is $\langle 100\rangle$.

REFERENCES

1. L. A. Maltseva, S. V. Grachev, T. V. Maltseva, and S. V. Yurin, RF Patent 2252977 (2005).
2. L. A. Maltseva, V. A. Sharapova, T. V. Maltseva, et al., RF Patent 2430187 (2011).
3. L. A. Mal'tseva, V. A. Zavalishin, S. B. Mikhailov, et al., "Properties of metastable steel 03Kh14N11K5M2YuT after thermoplastic treatment," Metalloved. Term. Obrab. Met. **51** (11–12), 557–562 (2009).
4. L. A. Mal'tseva, V. A. Sharapova, T. V. Maltseva, et al., "Effect of alloying and thermoplastic treatment on the phase composition and properties of corrosion-resistant steels with metastable austenite," Metalloved. Term. Obrab. Met. **53** (11–12), 529–537.
5. V. V. Grachev, A. V. Gromov, V. Ya. Tsellermaer, et al., "The evolution of dislocation substructures in small and medium-carbon steels at drawing," Vest. Samar. GTU, No. 27, 123–129 (2004).
6. A. M. Beese and D. Mohr, "Effect of stress triaxiality and Lode angle on the kinetics of strain-induced austenite-to-martensite transformation," Acta Materialia **59**, 2589–2600 (2011).
7. R. G. Stringfellow, D. M. Parks, and G. B. Olson, "A constitutive model for transformation plasticity accompanying strain-induced martensitic transformations in metastable austenitic steels," Acta Metallurgica et Materialia **40** (7), 1703–1716 (1992).
8. Heung Nam Han, Chang Gil Lee, Chang-Seok Oh, et al., "A model for deformation behavior and mechanically induced martensitic transformation of metastable austenitic steel," Acta Materialia **52**, 5203–5214 (2004).
9. Zhao-Hong Zhuang, Seok-Jae Lee, Young-Kook Lee, et al., "Effects of applied stresses on martensite transformation in AISI4340 steel," J. Iron Steel Res. Int. **14** (6), 63–67 (2007).
10. E. V. Shelekhov and T. A. Sviridova "Programs for X-ray analysis of polycrystals," Met. Sci. Heat Treatment **42** (7), 309–313 (2001).
11. K. Spencer, J. D. Embury, K. T. Conlon, et al., "Strengthening via the formation of strain-induced martensite in stainless steels," Mater. Sci. Eng., Ser. A **387–389**, 873–881 (2004).
12. R. K. Chin and P. S. Steif, "A computational study of strain inhomogeneity in wire drawing," Int. J. Mach. Tools Manufact. **35** (8), 1187–1198 (1995).